Evaporation of particle-stabilised emulsion sunscreen films.

Journal:	*ACS Applied Materials & Interfaces*
Manuscript ID	am-2016-063105.R1
Manuscript Type:	Article
Date Submitted by the Author:	n/a
Complete List of Authors:	Binks, Bernard; University of Hull, Chemistry Fletcher, Paul; University of Hull, Chemistry Johnson, Andrew; University of Hull, Chemistry Marinopoulos, Ioannis; University of Hull, Chemistry Crowther, Jonathan; GSK Consumer Healthcare (UK) Ltd. Thompson, Michael; GSK Consumer Healthcare

Evaporation of particle-stabilised emulsion sunscreen films.

Bernard P. Binks[a], Paul D.I. Fletcher[a]*, Andrew J. Johnson[a], Ioannis Marinopoulos[a], Jonathan M. Crowther[b] and Michael A. Thompson[c]

[o]*Department of Chemistry, University of Hull, Hull HU6 7RX, UK*
[b] *GSK Consumer Healthcare (UK) Ltd., 980 Great West Road, Brentford, Middlesex, TW8 9GS, UK*
[c]*GSK Consumer Healthcare, 184 Liberty Corner Rd, Warren, New Jersey, 07059, USA*

ABSTRACT

We recently showed (Binks *et al*., *ACS Appl. Mater. Interfaces*, **2016**, DOI: 10.1021/acsami.6b02696) how evaporation of sunscreen films consisting of solutions of molecular UV filters leads to loss of UV light absorption and derived sun protection factor (SPF). In the present work, we investigate evaporation-induced effects for sunscreen films consisting of particle-stabilised emulsions containing a dissolved UV filter. The emulsions contained either droplets of propylene glycol (PG) in squalane (SQ), droplets of SQ in PG or droplets of decane in PG. In these different emulsion types, the SQ is involatile and shows no evaporation, the PG is volatile and evaporates relatively slowly, whereas the decane is relatively very volatile and evaporates quickly. We have measured the film mass and area, optical micrographs of the film structure and the UV absorbance spectra during evaporation. For emulsion films containing the involatile SQ, evaporation of the PG causes collapse of the emulsion structure with some loss of specular UV absorbance due to light scattering. However, for these emulsions with droplets much larger than the wavelength of light, the light is scattered only at small forward angles so does not contribute to the diffuse absorbance and the film SPF. The UV filter remains soluble throughout the evaporation and thus the UV absorption by the filter and the SPF remain approximately constant. Both PG-in-SQ and SQ-in-PG films behave similarly and do not show area shrinkage by dewetting. In contrast, the decane-in-PG film shows rapid evaporative loss of the decane, followed by slower loss of the PG resulting in precipitation of the UV filter and film area shrinkage by dewetting which cause the UV absorbance and derived SPF to decrease. Measured UV spectra during evaporation are in reasonable agreement with spectra calculated using models discussed here.

KEYWORDS: sunscreen, evaporation, emulsion, spectrophotometry, precipitation, SPF

1. INTRODUCTION

Thin films of sunscreen formulations containing one or more molecular UV filters and/or metal oxide semiconductor particles are used to protect people from solar UV radiation. The initial mean thickness of a sunscreen film applied on to skin at a typical application rate of 1-2 mg cm^{-2} is generally in the range 10-20 μm. Different types of sunscreen formulations include simple solutions of molecular UV filters, dispersions of solid inorganic particles in a solvent and emulsions consisting of one immiscible liquid dispersed in a second. Simple solution films reduce UV light transmission only by absorption of the incident light whereas particle dispersions and emulsion films both absorb and scatter the incident light. Film transmission losses due to reflection are generally small for all the common types of sunscreen films.

The effectiveness of a sunscreen film may be quantified in terms of the sun protection factor (SPF) according to:

$$SPF = \frac{med_{with\ sunscreen}}{med_{without\ sunscreen}} \quad (1)$$

where med, with the appropriate subscript, is the minimum dose of sunlight which induces erythema (sunburn) in the presence or absence of the sunscreen film. Reliable estimation of SPF requires expensive and time-consuming *in vivo* measurements. However, SPF can be estimated *in vitro* by measuring the diffuse transmittance T of the sunscreen film as a function of the wavelength λ of the incident light. Measurements of T(λ) yield the film SPF according to:

$$SPF = \frac{\int_{290}^{400} E(\lambda)S(\lambda)d\lambda}{\int_{290}^{400} E(\lambda)S(\lambda)T(\lambda)d\lambda} \quad (2)$$

Literature values of the erythema action spectrum E(λ) and the spectral irradiance of terrestrial sunlight under defined conditions S(λ) combined with the measured T(λ) for a sunscreen film enables estimation of the film SPF[1-5]. In equation 2, the wavelength integration limits correspond to the SPF over the combined UVB and UVA wavelength ranges. Alternative SPF values corresponding to the separate UVB (290-320 nm) or UVA (320-400 nm) ranges[4] are simply derived by substitution of the appropriate wavelength integration limits. The SPF calculations presented here used tabulated values of E(λ) and S(λ) from reference 1 interpolated to give values at 1 nm wavelength intervals. The solar spectral irradiance S(λ) corresponds to midday midsummer sunlight for Southern Europe (latitude 40°N, solar zenith angle 20° and ozone layer thickness 0.305cm).

As noted above, one can make an *in vitro* measurement of T(λ) for an individual sunscreen film and use equation 2 to derive the corresponding SPF. However, for the purposes of developing new sunscreen formulations, it is much more useful to measure the extinction coefficient spectra of the relevant UV filters and then use the Beer-Lambert law to predict the absorbance spectrum for any film of defined initial thickness and set of initial concentrations of the relevant UV filters. The predicted absorbance yields T(λ) from which the predicted SPF is derived. This procedure, based on *in vitro* measurements of the extinction coefficient spectra of the UV filters, is a useful tool to predict SPF for different formulations of sunscreen films consisting of simple solutions of UV filters. However, SPF predictions made this way can differ considerably from *in vivo* measured values. Predicted

SPF estimations correspond to the *initial* state of the sunscreen film under test whereas *in vivo* SPF values correspond to time-averaged values over typical sunlight exposure times of a few hours. Hence, processes which alter the sunscreen film over time cause predicted SPF estimates to differ from the true, *in vivo* SPF values. Time-dependent SPF values can result from three main processes: (i) photochemical changes in the sunscreen film as a result of solar irradiation[6-9]; (ii) sunscreen film changes due to water immersion[10]; and (iii) evaporation of the volatile film components[11] which is the focus of this work. In a recent paper[12], we investigated the evaporation of thin sunscreen films consisting of solutions of molecular UV filters in a volatile solvent. Measurements of film mass and area as a function of evaporation time were used to model the evolution over time of the film spectra and derived SPF. Model calculations were in reasonable agreement with measured film spectra and derived SPF changes due to evaporation. Overall, it was demonstrated that film evaporation can alter the SPF by three mechanisms. Firstly, the film area can decrease by dewetting leading to a transient increase in the average film thickness (resulting in absorbance increase) and incomplete film coverage of the illuminated area (resulting in a decrease in absorbance). Secondly, the film thins by evaporative loss of the solvent which also causes the concentration of the ingredients to increase. These competing effects cause no net change in film absorbance. Thirdly, precipitation of the UV filter occurs when solvent loss causes the solubility limit to be reached. This precipitation results in a decrease in film absorbance since the precipitated UV filter does not contribute significantly to the overall film absorbance. Depending on the interplay of the three evaporation-induced effects, the UV absorbance of the film can sometimes show an initial transient increase due to film thickening driven by dewetting. However, at longer times, film evaporation causes a progressive loss of absorbance with a resultant decrease in SPF.

Reference 12 details the evaporation-induced changes in films initially consisting of *single-phase solutions* of a UV filter. However, many commercial sunscreen formulations consist of one or more UV filters dissolved or dispersed in an emulsion which is a thermodynamically-unstable dispersion of one liquid in a second immiscible liquid. Emulsions can be kinetically stabilised using either surfactants, polymers or small particles which adsorb at the liquid-liquid interface. In this study, we have investigated particle-stabilised emulsions containing the slowly-evaporating liquid propylene glycol (PG) as the polar phase and either involatile squalane (SQ) or rapidly evaporating n-decane as the apolar, "oil" phase. All emulsions contained a molecular UV filter which was soluble to different extents in both liquid phases of the emulsions. We show how film evaporation affects the UV spectrum and SPF for PG-in-SQ, SQ-in-PG and decane-in-PG emulsion types containing a UV filter.

2. EXPERIMENTAL

2.1 Materials. 4-*tert*-butyl-4'-methoxy dibenzoyl methane (AVB, Avobenzone, Sigma-Aldrich, pharmaceutical secondary standard) and *iso*-pentyl p-methoxycinnamate (MC, Neo Heliopan E1000, donated by the industrial sponsor GSK) were used as received. The UV extinction coefficient spectra in the solvents used here are shown in Figure 1. It was checked that each UV/filter/solvent system obeyed the Beer-Lambert law by measuring absorbance versus wavelength for a range of different concentrations and path lengths, converting them to extinction coefficient versus wavelength and checking that constant values of extinction coefficient were obtained for all concentrations, i.e. absorbance is proportional to concentration and path length. For path lengths in the range 0.001 to 1 cm and concentrations ranging from 0.045 to 9.61 mM, it was found that all extinction coefficients agreed within the estimated experimental uncertainty of a few %. Figure 1 shows the final averaged values of

extinction coefficient versus wavelength. Squalane (Sigma-Aldrich, 99% purity) was further purified by columning over neutral aluminium oxide (Merck) prior to use. Propan-1,2-diol (PG, Sigma-Aldrich, > 99%) and n-decane (TCI Europe, >99%) were used as received. Surface modified silica particles of primary particle diameters 10-30 nm (but containing aggregates of larger sizes) were provided by Wacker-Chemie (Germany). The surface modification consisted of chemical reaction of the silica surface silanol groups with dichlorodimethylsilane (DCDMS) to different extents. Particle samples with either 23% (most hydrophobic) or 35% unmodified SiOH surface groups were used here to stabilise the emulsions.

2.2 Methods. Equilibrium solubilities at 32^{o}C of AVB and MC in PG, SQ and decane were determined as described in ref. 12. The final values of the solubilities (Table 1) were the average of four measurements and are estimated to be accurate within approximately $\pm$10%.

Emulsions containing a UV filter were prepared as follows. Prior to emulsification, the required concentrations of the UV filter were dissolved in the polar (PG) and/or the apolar (SQ or decane) phases of the emulsion. Approximately equal (but accurately measured) volumes of the apolar and polar phases plus the required mass of dry silica particle stabilisers were emulsified in glass vessels (28 mm diameter by 72 mm height) at room temperature (21^{o}C) using an IKA Ultra – Turrax T25 homogeniser device equipped with a rotor-stator head of diameter 18 mm and operated at 13,000 rpm for 2 minutes. For particle-stabilised emulsions containing equal volumes of the two immiscible liquids, the emulsion type is controlled by the hydrophobicity of the stabilising particles. As noted above, we use silica particles hydrophobised to different extents. The silica particle hydrophobicity is indicated by the % of unmodified surface SiOH groups present; 100 %SiOH corresponds to maximum hydrophilicity and lower %SiOH correspond to increased hydrophobicity. For the emulsions used here containing equal volumes of the two immiscible liquids, 1 wt% of 23% SiOH silica particles produces PG-in-SQ emulsions, 1 wt% of 35% SiOH silica particles produces SQ-in-PG emulsions and 1 wt% of 23 %SiOH produces decane-in-PG emulsions. Emulsion type was determined using the "drop test" in which a drop of each pure liquid is added to the emulsion. A drop of the continuous phase liquid is observed to disperse in the emulsion whereas a drop of the emulsion droplet phase liquid does not disperse but remains as an isolated drop in the emulsion. Thus, the continuous and droplet phase of the emulsion is determined.

Films were prepared by depositing approximately 11 μL (approximately 12 mg) of the liquid film material on a quartz plate substrate (Hellma QS quartz Suprasil) with dimensions of 4.5 x 1.25 cm. The quartz plate was measured to have an optical transmittance of >90% with respect to air as reference over the wavelength range 200-400 nm. This transmittance corresponds to an absorbance of approximately 0.035 and is mainly due to light reflection at the quartz plate-air surfaces. An Eppendorf pipette was used to spread the sample as evenly as possible over an initial surface area of a few cm^2 to produce a film of initial mean thickness of a few tens of μm. The film was placed on a Linkam Peltier heating stage set to skin surface temperature of 32^{o}C and allowed to evaporate in the open lab air. During evaporation, the film mass was recorded at set times using a Denver instruments balance which was accurate to $\pm$0.2 mg. The film area and appearance were recorded using optical microscopy and the film absorption spectrum measured. Optical micrographs were obtained using an Olympus BX51 transmission microscope equipped with an Olympus DP 70 digital camera. Low magnification micrographs of the films were analysed using ImageJ software to determine the film perimeter and derive the total film area. For each set time, the average

film thickness d was derived from the measured values of film mass m and area occupied by the film A_{film} according to: $d = m/(A_{film}\,\rho)$ where ρ is the density of the film material. High magnification images of selected films containing precipitated crystals were also recorded.

Specular UV-vis spectra of the films were measured using a vertically-oriented Unicam UV3 UV/vis double beam spectrophotometer which enabled horizontal placement of the sample films (required to prevent unwanted film flow). This spectrophotometer records the *specular* optical transmittance over a small angular range with respect to the direction of the incident light (normal to the sample); any *diffuse* transmittance outside the angular range of the detector is not recorded. The angular range of light detected by the instrument detector is not known exactly but, from inspection of the optical arrangement, is estimated to be $\pm<5^o$ with respect to the incident beam direction. The position and area (1.6 cm x 0.2 cm = 0.32 cm^2) of the illuminated region on the sample was measured and kept constant for all samples. All film + substrate spectra were initially measured using only air in the reference beam of the spectrophotometer. The reference spectrum of the sunscreen film lacking the UV filter on the relevant substrate was measured separately (again using only air in the reference beam). The substrate reference spectrum was subtracted from the film + substrate spectrum to obtain the final spectrum of the film alone. All UV spectra reported here correspond to specular measurements unless noted otherwise.

Diffuse spectrophotometric measurements were made using a modified Horiba Scientific Fluoromax 4 instrument configured to allow horizontal mounting of the sample and equipped with an integrating sphere (Thorlabs) located directly underneath the sample and connected to the silicon detector of the Fluoromax 4. This instrument enabled measurement of the diffuse transmittance (and the corresponding absorbance) of the sample over a detector acceptance angular range of $\pm 60^o$ with respect to the incident light direction (normal to the sample) over the UV wavelength range 250-400 nm. Diffuse transmittance measurements using broad band incident light with a monochromator only on the detection side can potentially be distorted by sample fluorescence. Significant sample fluorescence is expected to cause negative apparent absorbance values (relative to the reference sample) at wavelengths higher than the sample absorption peaks. As seen in SI Figure 1, the high wavelength diffuse absorbance values of emulsion films with and without absorbing species are not significantly different. Hence, it is concluded that possible complications due to fluorescence are not significant here.

3. RESULTS AND DISCUSSION

This section is organised as follows. We first discuss the evaporation behaviour of films of AVB solutions in either PG or SQ. Section 3.2 shows the behaviour of emulsion films containing a UV filter, the involatile SQ and the slowly-evaporating PG. The behaviour of PG-in-SQ and SQ-in-PG emulsion types are measured and compared with model calculations. Finally, in section 3.3, we show the behaviour of emulsion films containing a UV filter, a rapidly-evaporating oil (decane) and slowly-evaporating PG.

3.1 Evaporation of solutions of AVB in PG and SQ. Figure 2 compares the variation of film mass, area, average thickness and illuminated area fraction for films of 8 mM AVB in either PG (which evaporates slowly) or SQ (which is totally involatile). As discussed in detail in ref. 12, the PG film dewets causing the area to shrink and the average film thickness to increase initially. The area shrinkage also causes the illuminated area fraction A_f to decrease below unity during the progressive mass loss by evaporation. Loss of PG solvent

causes the AVB to precipitate after 185 minutes, indicated by the vertical dashed line. In contrast, the involatile SQ film shows zero mass loss, only minor area decrease due to dewetting and no precipitation of the AVB.

Changes in the film peak absorbance values (at around 360 nm wavelength) resulting from evaporation of the two solvent films are compared in Figure 3. For the PG film, the interplay of the changes in film mass, area, thickness and A_f cause the peak absorbance due to AVB to initially increase and then decrease to around 20% of its initial value. Because of its involatility, the peak absorbance of the SQ film shows only minor changes over 24 hours.

3.2 Evaporation of PG-in-SQ and SQ-in-PG emulsion films containing either AVB or MC. These emulsions, containing equal volumes of PG and SQ, were prepared as described in the experimental section and spread on quartz plates. In the absence of evaporation, both emulsions were stable with respect to droplet coalescence for up to 2 years but did show creaming or sedimentation of the droplets. The AVB was added initially as an 8 mM solution in PG prior to emulsification. Following emulsification, the overall AVB concentration (expressed as moles per total volume of emulsion) was 4 mM. Within the emulsion, the AVB is expected to distribute between the PG and SQ phases with partition coefficient $P_{SQ/PG}$ given by the ratio of the AVB solubilities in the two solvents.

$$P_{SQ/PG} = \frac{[AVB]_{SQ}}{[AVB]_{PG}} = \frac{S_{SQ}}{S_{PG}} \qquad 3$$

where [AVB] and S are the equilibrium AVB concentrations and solubilities in each liquid phase of the emulsion, indicated by the subscript. From the solubility values in Table 1, AVB partitions in favour of the SQ phase with $P_{SQ/PG} = 38/14 = 2.7$. Using mass balance and equation 3, the overall and individual phase concentrations of AVB are related according to

$$[AVB]_{ov} = \phi_{SQ}[AVB]_{SQ} + \phi_{PG}[AVB]_{PG} = \left(\phi_{SQ}P_{SQ/PG} + \phi_{PG}\right)[AVB]_{PG} \qquad 4$$

where ϕ is the volume fraction of the phase indicated by the subscript. In equation 4, we have not included the volume fraction of stabilising particles in the emulsions since this is negligibly small (<0.01 initially). If it is assumed that the distribution of AVB equilibrates rapidly relative to the evaporation, equation 4 enables the calculation of the changing individual phase concentrations of AVB as ϕ_{PG} decreases due to evaporation. For the emulsions discussed here, it is likely that the AVB achieves its equilibrium distribution during the high shear emulsification process. In this case, the AVB concentrations in the two liquid phases at distribution equilibrium are $[AVB]_{PG} = 2.16$ mM and $[AVB]_{SQ} = 5.85$ mM prior to evaporation. In general, precipitation of the solute will occur when its concentration in one of the phases reaches its solubility in that phase. However, for the emulsions discussed below, the maximum AVB concentration reached in the SQ phase when all PG has evaporated is 8 mM. This is below the solubility limit and so precipitation of the AVB is not expected to occur, even when all the PG has evaporated.

Figure 4 shows the variation of film mass, area and derived average thickness with evaporation time for both PG-in-SQ and SQ-in-PG emulsion films. It can be seen that both emulsion films initially lose mass due to PG evaporation at similar rates. The initial mass loss rate is slightly faster for the PG-in-SQ film as compared with the SQ-in-PG film. However, the area of the PG-in-SQ film is slightly larger and so the mass loss rates *per unit area* of both films are not significantly different. Once the mass decreases to approximately

half its initial value corresponding to loss of all the initial PG, the mass of the residue SQ film remains constant. Both emulsion films show no decrease in area due to dewetting and the illuminated area fraction A_f (not shown here) remains equal to 1 throughout.

At first sight, it may appear surprising that the rate of PG loss from the emulsions is similar for films containing PG droplets within an involatile SQ continuous phase and for films where PG is the continuous phase. Previous studies of the evaporation of emulsions provides possible explanations[13-17]. For emulsions which consist of two liquid phases, the *equilibrium* vapour pressures of both liquid phases (assuming complete mutual immiscibility) are identical to the equilibrium vapour pressures of the individual pure liquids. As discussed in ref. 13, under conditions in which the rate limiting step for evaporation is the rate of diffusion of vapour molecules across a "stagnant" gaseous layer immediately above the liquid surface, the evaporation rate is proportional to the equilibrium vapour pressure. Under these conditions, both the droplet and continuous phase liquids of an emulsion will evaporate at the same rate as the pure liquids under the same conditions. For the continuous phase liquid of emulsions, it has been shown that the presence of adsorbed films of emulsifiers at the emulsion-vapour surface do not impose significant resistance to evaporation and hence the evaporation rate of the continuous phase is virtually identical to that of the pure liquid[13]. For the droplet phase liquid of an emulsion, the rate limiting step for evaporation can switch to one of two possibilities. Firstly, entry and/or spreading of the droplets at the emulsion-vapour surface can be rate limiting. Secondly, if droplet entry into the emulsion-vapour surface does not occur (i.e. a thin layer of continuous phase always separates the droplets from the vapour phase), the rate limiting step can be droplet phase dissolution followed by dissolved molecule diffusion across the thin film of continuous phase separating the droplets from the vapour phase. It has been shown[13] that oil droplet evaporation from surfactant-stabilised oil-in-water emulsions occurs with this latter rate limiting step for oils which have a very low solubility in the water continuous phase. For droplet-dispersed oils with high solubility in the emulsion continuous phase, mass transport to the emulsion-vapour surface is fast and the rate limiting step reverts to diffusion across the stagnant vapour layer. The result is that droplet phases which are relatively soluble in the continuous phase evaporate with the same rate as the pure droplet liquid whereas non-entering droplet phases with low solubility in the continuous phase can evaporate more slowly. For the emulsions containing PG and SQ, we observe that the PG evaporates at similar rates when present as either the continuous or droplet phase and that both emulsion rates are similar to that for pure PG. Although we have not measured the solubility of PG in squalane at 32^{o}C, we note that the solubility of PG in mineral oil (which is chemically similar to squalane) at 20^{o}C is relatively high (0.31 ± 0.06 wt%)[18]. Hence, if PG droplet entry does not occur, PG droplets are expected to evaporate at a rate similar to PG as continuous phase and pure PG, as observed here.

Figures 5 and 6 show the evolution of the droplet structure during PG evaporation from thin films of PG-in-SQ and SQ-in-PG emulsions respectively. For the PG-in-SQ emulsion film (Figure 5), the initial mean droplet diameter is approximately 20 μm and the mean initial film thickness is approximately 65 μm so at time = 0 minutes, a multilayer of emulsion drops is seen, i.e. drops on top of drops. As evaporation proceeds and the volume fraction of PG decreases, the apparent mean drop diameter increases and the PG droplets decrease in concentration so that only a monolayer of droplets is observed after 100 minutes. The more dense PG droplets are expected to sediment to the quartz plate and may partially wet it to form a layer of adhering PG lenses under a covering layer of SQ (micrographs at 120 and 140 minutes). Continued evaporation of the PG then leaves a filigree pattern of silica particle/PG residues (160 minutes) which finally loses visibility by 180 minutes. Although

other interpretations of the structure images (e.g. catastrophic phase inversion from PG-in-SQ to SQ-in-PG) cannot be rigorously excluded, the scenario described above provides a plausible interpretation of the images of Figure 5. For the SQ-in-PG emulsion film (Figure 6), the initial mean SQ droplet diameter is approximately 30 μm. Evaporation of the PG continuous phase causes progressive concentration of the droplets until a high internal phase emulsion (HIPE) containing non-spherical droplets is obtained at 100 minutes when ϕ_{PG} is 0.31. Further PG evaporation from the thin lamellae separating the SQ droplets again leads to a filigree pattern of silica particle/PG residues (120 minutes) which loses visibility by 140 minutes.

Figures 7 and 8 show the evolution of the UV spectra (versus air as reference) of PG-in-SQ and SQ-in-PG films containing AVB on a quartz plate with evaporation time. For both emulsion types, the peak absorbance at approximately 360 nm increases slightly over the first 30 minutes or so, decreases for 100-250 minutes and then remains approximately constant.

In general, loss of light transmittance by these types of emulsion film results from a combination of three processes: absorption by the UV filter (assuming no absorption by the solvents or other components as is the case in this study), scattering from the emulsion structure and reflection from the interfaces of the emulsion and quartz plate. The measured optical absorbance A (equal to $-\log_{10}T$ where T is the fraction of incident light transmitted) is taken to be the sum of three contributions:

$$A = A_{abs} + A_{scat} + A_{reflect} \quad (5)$$

where A_{abs} is the absorbance due to absorption (by AVB in this case), A_{scat} is the absorbance resulting from light scattering by the emulsion and $A_{reflect}$ is the absorbance contribution from reflection losses from the emulsion and quartz plate surfaces. Note that equation 5 is an approximation since, in general, (i) the absorption properties of particles such as the emulsion droplets can affect their scattering properties[19] and (ii) multiple scattering of light through a light-absorbing continuous phase can cause an increase in absorption due to the increased effective path length taken by multiply-scattered light[20]. This latter effect is only significant when the absorbance contribution due to scattering is more than approximately 3 times larger than the contribution due to absorption. This is not the case here and so this effect is not relevant here. As seen later, the possible complicating effect of (i) also does not appear to be significant here and so the use of equation 5 is justified *a postiori*.

The values of $A_{reflect}$ for either a bare quartz plate or plates with films of either pure PG or pure SQ were all approximately equal to 0.035 and wavelength independent. Over the wavelength range of interest, the absorption contribution A_{abs} results from light absorption by the dissolved UV filter. Solutions of the UV filters used here follow the Beer-Lambert law

$$A_{abs} = \varepsilon[UV\ filter]d \quad (6)$$

where d is the path length and ε is the molar extinction coefficient (wavelength and solvent dependent, see Figure 1) and [UV filter] is the concentration of the UV filter. For evaporating emulsion films containing PG and SQ as solvents and AVB as the UV filter, the volume fractions of both solvents, the concentrations of UV filter in each solvent and the path length (equal to film thickness) all change with evaporation time. The contribution to the overall absorbance from absorption by the UV filter is

$$A_{abs} = d\left(\phi_{SQ}[AVB]_{SQ}\varepsilon_{SQ} + \phi_{PG}[AVB]_{PG}\,\varepsilon_{PG}\right) \quad (7)$$

where the subscripts indicate the solvent phase. Equation 7 is valid under conditions when the spatial distribution of the UV filter is uniform over the area illuminated during the absorbance measurement. There has been extensive literature discussion of how film non-uniformity, mainly taken as point-to-point variation in film thickness, affects the apparent optical absorbance of the film[21-26]. For a film which is non-uniform in either thickness or light transmittance at different positions within the illuminated film area, the measured optical absorbance is equal to the negative logarithm of the film transmittance averaged over the illuminated film area. Hence for equation 7 to be valid, the film must cover the illuminated area, i.e. $A_f = 1$ which is the case for the measured spectra of Figures 7 and 8 throughout the evaporation. Within the emulsion films, the AVB concentration is non-uniform as a result of AVB partitioning between the droplet and continuous phases. However, the amount of AVB per unit film area will be reasonably uniform so long as the emulsion drops are small relative to the film thickness and present at greater than monolayer coverage. This is the case for the emulsion films in the initial stages of the evaporation. When all the PG has evaporated, the AVB is uniformly distributed with the SQ phase over the film area. At intermediate evaporation times, significant non-uniformity of the AVB distribution from point to point within the film cannot be rigorously excluded and so equation 7 must be regarded as approximate in this time period.

The emulsion films scatter light. When measured using the specular spectrophotometer versus air as reference, the specular absorbance (mainly due to scattering) of a 100 μm thickness PG-in-SQ emulsion film containing no UV filter is 0.7-1.0 and only weakly dependent on wavelength (Figure S1). Comparison with the specular absorbance spectrum of identical emulsion films containing either AVB or MC shows that the absorbance due to the UV filters adds to the specular absorbance contribution due to scattering which is approximately wavelength independent and similar in magnitude to the absorbance of the films at a wavelength of 400 nm where the extinction coefficients of the UV filters are zero. The specular spectra are compared with the diffuse spectra recorded for the same films. For the emulsion film with no UV filter, it can be seen that the diffuse absorbance versus air as reference is not significantly different to $A_{reflect}$ (approx. 0.035), i.e. the *diffuse* absorbance due to scattering is virtually zero. For films containing a UV filter, the diffuse absorbance contribution due to absorption again adds to the absorbance of the emulsion film alone. This result indicates that the scattered light intensity is fully transmitted through the sample film and is all detected by the diffuse spectrophotometer with a detector acceptance angular range of $\pm 60^o$. When measured using the specular instrument, some of the transmitted scattered light intensity falls outside the detector acceptance angular range ($\pm < 5^o$) and the specular instrument thus records a non-zero absorbance due to scattering. Importantly for sunscreen films, the SPF is determined by the fraction of light transmitted over an angular range of $\pm 90^o$ with respect to normal incident light. Hence, for the emulsion films considered here for which the diffuse $A_{scat} = 0$, the non-zero values of A_{scat} recorded on the specular instrument do *not* contribute to the SPF.

Some additional insights into the scattering from these emulsion films can be drawn from theoretical calculations. Using software from ref. 27, we have calculated the scattering efficiency Q_{scat} corresponding to non-interacting, non-multiply scattering emulsion droplets of 10 μm mean radius and 30% polydispersity as a function of wavelength. For these calculations, the refractive index values of the solvents (Table S1, data from refs. 28-34) were

taken to be wavelength independent since the wavelength dependence was not available. Scattering efficiency values were converted to A_{scat} values using[35]

$$A_{scat} = \frac{3\phi_{drops}Q_{scat}d}{4ln(10)\langle r\rangle} \quad 8$$

where ϕ_{drops} is the volume fraction of emulsion droplets and <r> is the mean droplet radius. In addition to neglecting droplet interactions and multiple scattering, values of A_{scat} estimated using equation 8 correspond to the situation in which all scattering intensity is assumed to contribute to the overall loss in transmittance. As shown in the upper plot of Figure S2, the absorbance due to scattering is only weakly dependent on wavelength. The calculated scattering angle dependence of the scattering intensity at fixed wavelength of 300 nm is shown in the lower plot of Figure S2 where it can be seen that the light is strongly forward scattered within an angular range of $\pm 2^o$ with respect to the incident light direction. Similar angular dependences (not shown) are calculated for all wavelengths in the range 200-400 nm. Despite neglecting the effects of droplet interactions, multiple scattering and the wavelength dependences of the refractive index values of the solvents, the calculations indicate that (i) these emulsion films scatter light only at small scattering angles; (ii) A_{scat} is only weakly dependent on wavelength and (iii) the calculated values of A_{scat} are much larger than the apparent values measured using either a specular or diffuse spectrophotometer instrument. It appears that the specular instrument used here with a detector angular range of $\pm<5^o$ detects most of the forward scattered light and hence reports only a small fraction of the total absorbance due to scattering. The diffuse spectrophotometer with a detector angular of $\pm 60^o$ detects virtually all the scattered light intensity and so reports an absorbance contribution due to scattering of zero. The calculations are consistent with the experimental observations; overall, the light scattering from these emulsion films is strongly forward scattering and hence the scattering does not contribute to the SPF of these films. For all the model calculations described below, we take A_{scat} to be wavelength independent (since the Mie scattering calculations indicate only a slight wavelength dependence) and equal to the specular absorbance measured at 400 nm (since none of the UV filters used here absorb at this wavelength and so the measured absorbance is due solely to scattering).

Figures S3 and S4 show the variation of PG volume fraction and the specular absorbance due to scattering (A_{scat}, taken to be equal to the measured absorbance at 400 nm) with emulsion film evaporation time. In conjunction with the optical micrographs of Figures 5 and 6, it can be seen how the loss of PG by evaporation and the collapse of the emulsion droplet structure is related to the progressive decrease in A_{scat}.

Equations 5-7, together with the assumption that the specular A_{scat} is equal to the measured absorbance at 400 nm, enable the calculation of the specular emulsion film spectra as evaporation proceeds. As seen in Figures 7 and 8, calculated and measured spectra for both emulsion types are in reasonably good agreement. The largest spectral changes result from the decrease in the specular A_{scat} due to the collapse of the emulsion droplet structure. The changes in the absorbance contribution due to adsorption by AVB which occur as a result of the changing distribution of the AVB between the PG and SQ phases are minor as the AVB extinction coefficients in both solvents are quite similar (Figure 1). The calculated spectra were used to derive both the specular (i.e. including the specular A_{scat} contribution) and the diffuse SPF (for which the A_{scat} contribution is zero). It can be seen that the specular SPF values change with evaporation time whereas the diffuse SPF values are virtually constant. It is the diffuse SPF which corresponds to the true measure of the sunscreen

effectiveness. Although this comparison of SPF values derived from measured and calculated spectra serves to successfully validate the model, we note that the actual SPF values are small in comparison to values for commercial sunscreen products.

As seen in Figures S5 and S6, PG-in-SQ and SQ-in-PG emulsion films containing MC as UV filter behave similarly to the films containing AVB which are described above. Overall, for sunscreen emulsion films in which one liquid component is involatile and the UV filter remains fully soluble during evaporation, we conclude that the main changes in the specular spectra of these films due to film evaporation result mainly from the loss of light scattering due to the collapse of the emulsion structure. Because the light is strongly forward scattered, the diffuse spectra and the true SPF values of these films do not change significantly as a result of evaporation. In contrast to sunscreen films consisting of solutions in a volatile solvent, formulation of sunscreens within emulsions which contain an involatile component and in which the UV filter remains fully soluble successfully achieve an SPF which is not lost by evaporation.

3.3 Evaporation of decane-in-PG emulsion films containing AVB.

Evaporation of sunscreen films consisting of simple solutions of a UV filter causes precipitation of the UV filter and loss of UV absorption and SPF. In emulsion sunscreen films containing the involatile SQ, precipitation of the UV filter is prevented and loss of SPF by evaporation is avoided. However, the residue of involatile SQ remaining after evaporation may or may not be acceptable to consumers and so we have extended this study to include an emulsion sunscreen film in which both emulsified liquids evaporate. The emulsion consists of 50 vol% (initially) of decane droplets (which evaporate relatively fast) dispersed in a PG continuous phase (which evaporates relatively slowly). Prior to evaporation, the film contained 4 mM AVB for which evaporative loss of both solvents leads to precipitation.

Figure 9 shows the variation of film mass, area, average thickness and fraction of illuminated area (see Figure S7) covered during the complete evaporation of this emulsion film. There is a rapid initial loss of film mass which, unlike the SQ-containing emulsion films, is accompanied by a rapid film area contraction due to dewetting. The area contraction causes an initial thickening of the film which is then followed by a progressive decrease to zero film thickness. The film area contraction also causes the fraction of illuminated area to decrease below 1 in this case.

The equilibrium partition coefficient for AVB distribution between decane and PG is estimated from the solubility values in Table 1 to be $P_{decane/PG} = 3.9$. If equilibrium partitioning of AVB is maintained during evaporation of the emulsion films, the initial AVB concentration of 4 mM (with respect to the overall emulsion volume) is expected to first fully transfer to the PG phase as decane is lost to give an AVB concentration within the PG phase of 8 mM. Evaporative loss of PG causes the AVB concentration to increase to its solubility limit in PG (14 mM, Table 1), at which point precipitation of AVB is expected. Thus, *if the AVB partitioning maintains its equilibrium*, precipitation is expected to occur when the film mass has decreased to 0.0057 g which corresponds to approximately 180 minutes of evaporation. In fact, AVB precipitation in the emulsion films is first observed after only 20 minutes, corresponding to the point at which virtually all the decane has evaporated. It appears that the evaporation of the decane is sufficiently rapid such that the AVB in decane precipitates rather than transferring to the PG phase.

Figure 10 shows representative optical micrographs of the decane-in-PG emulsion film at different stages during the evaporation. In the absence of evaporation, micrographs (not shown here) within a sealed container show that the emulsion drop size remains approximately constant over 240 minutes. With evaporation, the decane droplets shrink rapidly and are lost within 20 minutes or so. The emulsion film dewets from the quartz plate substrate and shows patches of bare quartz plate substrate and areas covered with residual PG continuous phase. A patchy residue of precipitated AVB crystals develops progressively after about 20 minutes of evaporation.

Figure 11 shows the measured and calculated specular UV spectra of the decane-in-PG emulsion film during evaporation. The measured spectra shows an initial rapid decrease in AVB absorption (indicated by the peak at 360 nm) followed by a slower decrease in the peak height to zero. The specular absorbance due to film scattering (corresponding approximately to the absorbance value at 400 nm) varies with evaporation as shown in the middle plot of Figure 11. The changes presumably correspond to the effects of loss of the emulsion structure, the formation of the "patchy" film of PG and bare quartz substrate and the formation of the final residue of precipitated AVB crystals. The calculated UV spectra are based on equations 5-7 with the following additional assumptions. Firstly, it is assumed that the AVB does not partition significantly during the rapid evaporation of the decane. The AVB concentrations in each phase increase from their initial values (6.35 mM in decane and 1.65 mM in PG) until the solubility in each phase is reached and precipitation occurs. As detailed in ref. 12, the absorbance of each liquid phase is assumed to arise from only the *dissolved* AVB; the precipitated AVB is assumed to contribute zero absorbance. Finally, these decane-in-PG emulsion films shrink in area due to dewetting and the fraction of area illuminated in the spectrophotometric measurements A_f decreases to below unity. This latter effect is included in the calculations using

$$Abs_{measured} = -log_{10}\{A_f 10^{-Abs_{film}/A_f} + (1 - A_f)\} \quad (9)$$

where $Abs_{measured}$ is the measured value of absorbance resulting from a film of absorbance equal to Abs_{film} covering an illuminated area fraction A_f. The area fraction not covered by the film $(1 - A_f)$ is assumed to show zero absorbance. The model calculations correctly capture the observed rapid decrease followed by a slower progressive decrease in absorbance due to light absorption which decreases to virtually zero. However, the calculated short time increase in absorbance does not agree with the measured spectra. This may be a result of some inaccuracy in the exact extent of decane evaporation corresponding to the time at which the first spectrum was measured. Overall, it is clear that the film absorbance due to light absorption is fully lost by evaporation. It is also likely that the measured specular absorbance of the final film residue due to light scattering by the large particles remaining after evaporation corresponds to strongly forward scattering and so is not expected to contribute to the SPF. Hence, evaporation of emulsion films not containing an involatile component is expected to result in complete loss of film SPF.

4. CONCLUSIONS

In a previous publication[12], we have shown that complete evaporation of sunscreen films consisting of simple solutions of a UV filter in a solvent generally leads to loss of UV light absorption and reduction of the corresponding SPF over a timescale determined by the solvent evaporation rate. For solution sunscreen films, the decrease of SPF is a result of film area dewetting and/or precipitation of the UV filter. In the present work, we have shown that

when a UV filter is incorporated within an emulsion in which one of the emulsion liquids is involatile, the UV light absorption is retained during evaporation as precipitation of the UV filter is prevented. The specular absorbance of the emulsion films does decrease during evaporation because the optical transmittance of the films increases as evaporation causes loss of the emulsion structure, thereby decreasing light scattering. However, because the emulsion drops are large relative to the wavelength of the light, the light scattering occurs at small forward angles and so the scattering does not contribute to the diffuse absorbance of these films with the result that the film SPF is virtually unaffected by evaporation. For the particle-stabilised emulsion films containing PG (volatile) and SQ (involatile) investigated here, we observe that PG-in-SQ and SQ-in-PG emulsion films behave similarly. Unlike the solution sunscreen films, these emulsion films show no area shrinkage due to dewetting and so potential SPF losses due to this effect are also suppressed. For emulsion sunscreen films in which the involatile SQ is replaced by the volatile decane, evaporation of both emulsion liquids causes precipitation of the UV filter and virtually complete loss of UV light absorption. In addition, it is observed that the relatively rapid evaporation of the decane component from these emulsion films is accompanied by film area shrinkage due to dewetting. For all the emulsion films, the measured UV spectra during evaporation are reasonably well described by model calculations. Liquid evaporation rates, and hence the time scales over which evaporation-induced effects on sunscreen performance occur, are dependent on the properties of the particular liquids involved, particularly vapour pressure. Evaporation rates of candidate liquid components to be used in novel test formulations can either be measured or estimated as described in ref. 12 using the relevant liquid properties. In this way, findings from this study are easily transferable to sunscreen formulations using liquid components other than those used here. Overall, this study establishes the principles governing how emulsion formulations of sunscreen films can be designed to maximally retain their SPF during evaporation.

ASSOCIATED CONTENT

Table S1. Physical properties of PG, SQ and n-decane at 32^{o}C (data from refs. 28-34).

Figure S1. Comparison of the specular and diffuse UV spectra (all versus air as reference) of 100 μm path length PG-in-SQ emulsion films containing equal volumes of SQ and PG with and without AVB or MC. The films were stabilised using 1 wt% of 23% SiOH silica particles and the spectra were measured in closed cuvettes without evaporation. For the diffuse measurements, the instrument sensitivity limits the wavelength range to wavelengths greater than approximately 250 nm.

Figure S2. Upper plot: Calculated film absorbance due to scattering of PG-in-SQ and SQ-in-PG emulsion films of 100 μm thickness containing equal volumes of SQ and PG without UV filter. The calculations are for non-interacting droplets of mean radius 10 μm with a polydispersity (standard deviation/mean) of 30% with no multiple scattering. Lower plot: Scattering intensity (arbitrary units) versus scattering angle for the PG-in-SQ emulsion film at a wavelength of 300 nm.

Figure S3. Variation of the volume fraction of PG with evaporation time for PG-in-SQ and SQ-in-PG emulsion films initially containing approximately equal volumes of SQ and PG and 4 mM AVB in the total emulsion.

Figure S4. Variation of the specular absorbance at 400 nm wavelength with evaporation time for PG-in-SQ and SQ-in-PG emulsion films initially containing equal volumes of SQ and PG and 4 mM AVB in the total emulsion.

Figure S5. Measured (upper plot) and calculated (lower plot) UV spectra versus air as reference during evaporation of a PG-in-SQ emulsion film initially with 13.7 mg mass and containing equal volumes of SQ and PG and 4.19 mM MC in the total emulsion (initially dissolved in the PG phase). The film was stabilised using 1 wt% of 23% SiOH silica particles.

Figure S6. Measured (upper plot) and calculated (lower plot) UV spectra versus air as reference during evaporation of a SQ-in-PG emulsion film initially with 15.7 mg mass and containing equal volumes of SQ and PG and 4.19 mM MC in the total emulsion (initially dissolved in the PG phase). The film was stabilised using 1 wt% of 35% SiOH silica particles.

Figure S7. Overall film area images of an evaporating film of a decane-in-PG emulsion initially containing equal volumes of decane and PG with 4 mM AVB. The emulsion was stabilised by 1 wt% of 23% SiOH silica particles. The red rectangles show the area illuminated in the spectrophotometry measurements.

ACKNOWLEDGEMENTS

We thank GlaxoSmithKline Consumer Healthcare for funding this work and supplying the samples of UV filters used here. We also thank Dr. H. Snelling and Mr. A. Clarke of the Dept. of Physics, University of Hull for their help with the diffuse transmittance measurements.

REFERENCES

1. Diffey, B.L.; Robson, J. A New Substrate to Measure Sunscreen Protection Factors throughout the Ultraviolet Spectrum. *J. Soc. Cosmet. Chem*., **1989**, *40*, 127-133.
2. Diffey, B.L.; Tanner, P.R.; Matts, P.J.; Nash, F.J. In Vitro Assessment of the Broad-Spectrum Ultraviolet Protection of Sunscreen Products. *J. Amer. Acad. Dermatol*., **2000**, *43*, 1024-1035.
3. Osterwalder, U.; Herzog, B. Sun Protection Factors: World Wide Confusion. *Brit. J. Dermatol*. **2009**, *161*, 13-24.
4. Schmalwieser A.W.; Wallisch, S.; Diffey, B. A Library of Action Spectra for Erythema and Pigmentation. *Photochem. Photobiol. Sci*., **2012**, *11*, 251- 268.
5. Moyal, D.; Alard, V.; Bertin, C.; Boyer, F.; Brown, M.W.; Kolbe, L.; Matts, P.; Pissavini, M. The Revised COLIPA In Vitro UVA Method. *Int. J. Cosmetic Sci*., **2013**, *35*, 35-40.
6. Herzog, B.; Wehrle, M.; Quass, K. Photostability of UV Absorber Systems in Sunscreens. *Photochem. Photobiol.*, **2009**, *85*, 869-878.
7. Stanfield, J.; Osterwalder, U.; Herzog, B. In Vitro Measurements of Sunscreen Protection. *Photochem. Photobiol. Sci*., **2010**, *9*, 489-494.
8. Shaath, N.A. Ultraviolet Filters. *Photochem. Photobiol. Sci*., **2010**, *9*, 464-469.
9. Kockler, J.; Oelgemoller, M.; Robertson, S.; Glass, B.D. Photostability of Sunscreens. *J. Photochem. Photobiol. C*, **2012**, *13*, 91-110.
10. U.S. Department of Health and Human Services, Food and Drug Administration, Center for Drug Evaluation and Research (CDER), Guidance for Industry. Labeling and Effectiveness Testing: Sunscreen Drug Products for Over-The-Counter Human Use — Small Entity Compliance Guide, December **2012**.
11. Beyer, D.M.; Faurschou, A.; Philipsen, P.A.; Hoedersdal, M.; Wulf, H.C. Sun Protection Factor Persistence on Human Skin During a Day Without Physical Activity

or Ultraviolet Exposure. *Photodermatol. Photoimmunol & Photomed*., **2010**, *26*, 22-27.

12. Binks, B.P.; Brown, J.; Fletcher, P.D.I.; Johnson, A.J.; Marinopoulos, I.; Crowther, J.M.; Thompson, M.A. Evaporation of Sunscreen Films: how the UV Protection Properties Change. *ACS Appl. Mater. Interfaces*, **2016**, DOI: 10.1021/acsami.6b02696
13. Aranberri, I.; Beverley, K.J.; Binks, B.P.; Clint, J.H.; Fletcher, P.D.I. How do Emulsion Drops Evaporate? *Langmuir*, **2002**, *18*, 3471-3475.
14. Aranberri, I.; Binks, B.P.; Clint, J.H.; Fletcher, P.D.I. Retardation of Oil Drop Evaporation from Oil-in-Water Emulsions. *Chem. Commun*., **2003**, 2538-2539.
15. Aranberri, I.; Binks, B.P.; Clint, J.H.; Fletcher, P.D.I. Evaporation Rates of Water from Concentrated Oil-in-Water Emulsions. *Langmuir*, **2004**, *20*, 2069-2074.
16. Binks, B.P.; Fletcher, P.D.I.; Holt, B.L.; Beaussoubre, P.; Wong, K. Selective Retardation of Perfume Oil Evaporation from Oil-in-Water Emulsions Stabilized by either Surfactant or Nanoparticles. *Langmuir*, **2010**, *26*, 18024-18030.
17. Dunstan, T.S.; Fletcher, P.D.I.; Mashinchi, S. High Internal Phase Emulsions: Catastrophic Phase Inversion, Stability and Triggered-Destabilization. *Langmuir*, **2012**, *28*, 339-349.
18. Binks, B.P.; Fletcher, P.D.I.; Thompson, M.A.; Elliott, R.P. Effect of Added Diols (Glycols) on the Emulsion Properties of Oil, Water and Surfactant Mixtures. *Colloids Surf. A*, **2011**, *390*, 67-73.
19. Bohren, C.F.; Huffman, D.R. Absorption and Scattering of Light by Small Particles. Wiley-VCH, Weinheim, **2004**.
20. Herzog, B.; Sengün, F. Scattering Particles Increase Absorbance of Dyes – a Model Study with Relevance for Sunscreens. *Photochem. Photobiol. Sci.*, **2015**, *14*, 2054-2063.
21. O'Neill, J.J. Effect of Film Irregularities on Sunscreen Efficacy. *J. Pharm. Sci*., **1984**, *73*, 888-891.
22. Ferrero, L.; Pissavini, M.; Marguerie, S.; Zastrow, L. Efficiency of a Continuous Height Distribution Model of Sunscreen Film Geometry to Predict a Realistic Sun Protection Factor. *J. Cosmet. Sci*., **2003**, *54*, 463-481.
23. Herzog, B.; Mongiat, S.; Quass, K.; Deshayes, C. Prediction of Sun Protection Factors and UVA Parameters of Sunscreen by Using a Calibrated Step Film Model. *J. Pharm. Sci*., **2004**, *93*, 1780-1795.
24. Ferrero, L.; Pissavini, M.; Doucet, O. How a Calculated Model of Sunscreen Film Geometry can Explain In Vitro and In Vivo SPF Variation. *Photochem. Photobiol. Sci*., **2010**, *9*, 540-551.
25. Atkin, S.L.; Barrier, S.; Cui, Z-G.; Fletcher, P.D.I.; Mackenzie, G.; Panel, V.; Sol V.; Zhang. X. UV and Visible Light Screening by Individual Sporopollenin Exines Derived from Lycopodium Clavatum (Club Moss) and Ambrosia Trifida (Giant Ragweed). *J. Photochem. Photobiol. B*, **2011**, *102*, 209-217.
26. Herzog, B.; Osterwalder, U. Simulation of Sunscreen Performance. *Pure & Appl. Chem.*, **2015**, *87*, 937-951.
27. MiePlot version 4.5.01 downloaded from http://www.philiplaven.com/mieplot.htm
28. George, J.; Sastry, N.V. Densities, Dynamic Viscosities, Speeds of Sound and Relative Permittivities for Water + Alkanediols at Different Temperatures. *J. Chem. Eng. Data* **2003**, *48*, 1529-1539.
29. Stull, D.R. Vapor Pressures of Pure Substances. Organic Compounds. *Ind. Eng. Chem.*, **1947**, *39*, 517-540.
30. Fontao, M.J.; Iglesias, M. Effect of Temperature on the Refractive Index of Aliphatic Hydroxylic Mixtures. *Int. J. Thermophys.*, **2002**, *23*, 513-527.

31. Schmidt, K.A.G.; Pagnutti, D.; Curran, M.D.; Singh, A.; Trusler, J.P. M.; Maitland, G.C.; McBride-Wright, M. New Experimental Data and Reference Models for the Viscosity and Density of Squalane. *J. Chem. Eng. Data*, **2015**, *60*, 137-150.
32. VonNiederhausern, D.M.; Wilson, G.M.; Giles, N.F. Critical Point and Vapor Pressure Measurements at High Temperatures by Means of a New Apparatus with Ultralow Residence Times. *J. Chem. Eng. Data*, **2000**, *45*, 157-160.
33. Dubey, G.P.; Tripathi, N.; Bhatia, S.C. Refractive Index of Ternary Liquid Systems of Squalane (+ Hexane + Benzene; + Cyclohexane + Benzene and + Hexane + Cyclohexane). *Ind. J. Pure & Appl. Phys.*, **2005**, *43*, 175-179.
34. Selected Values of Properties of Hydrocarbons and Related Compounds. Haas, C.W. (Ed.), Thermodynamic Research Center, Texas A&M University, College Station, Texas, **1978**.
35. McClements, D.J. Theoretical Prediction of Emulsion Color. *Adv. Colloid Interface Sci.*, **2002**, *97*, 63-89.

Table 1. Solubilities of AVB and MC in different solvents at 32°C.

UV absorber	Solvent	Solubility/mM
AVB	propylene glycol	14
AVB	squalane	38
AVB	decane	54
MC	propylene glycol	435
MC	squalane	1300

Figure 1. Spectra of AVB (upper plot) and MC (lower plot) in different solvents at 32°C.

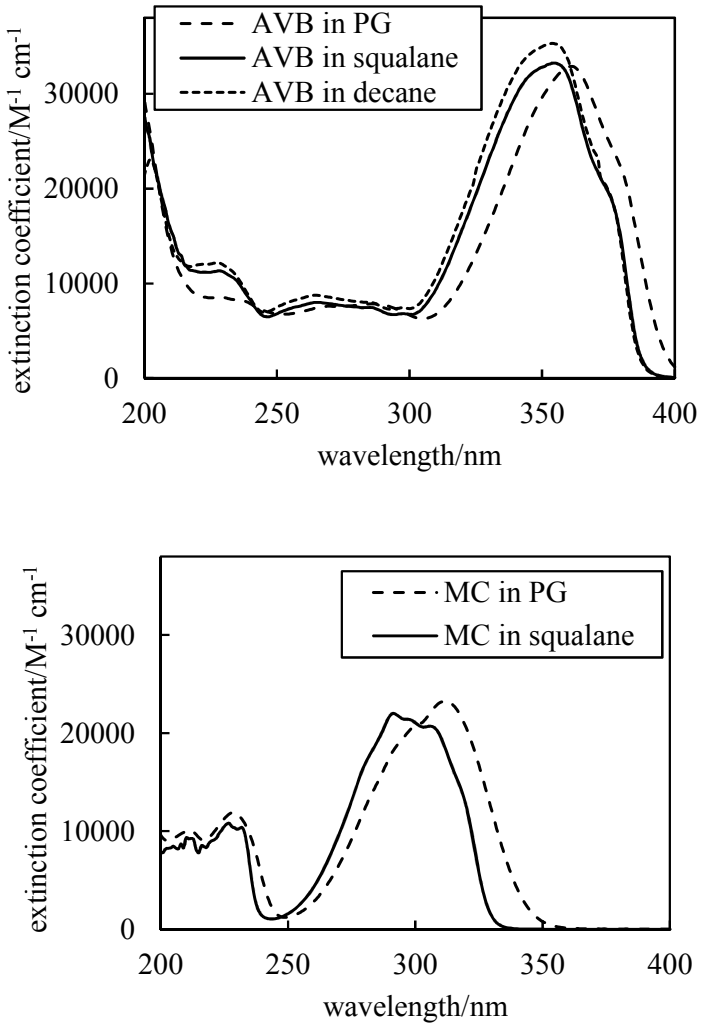

Figure 2. Variation of film mass, area, average thickness and fraction of illuminated area covered (A_f) with evaporation time for films containing 8 mM AVB in PG (open circles) and in squalane (filled circles). The horizontal dashed lines indicate the long-time behaviour of the squalane films (measured at 1440 min). In the film mass plot, the vertical dashed line indicates the time at which AVB precipitates in the PG film.

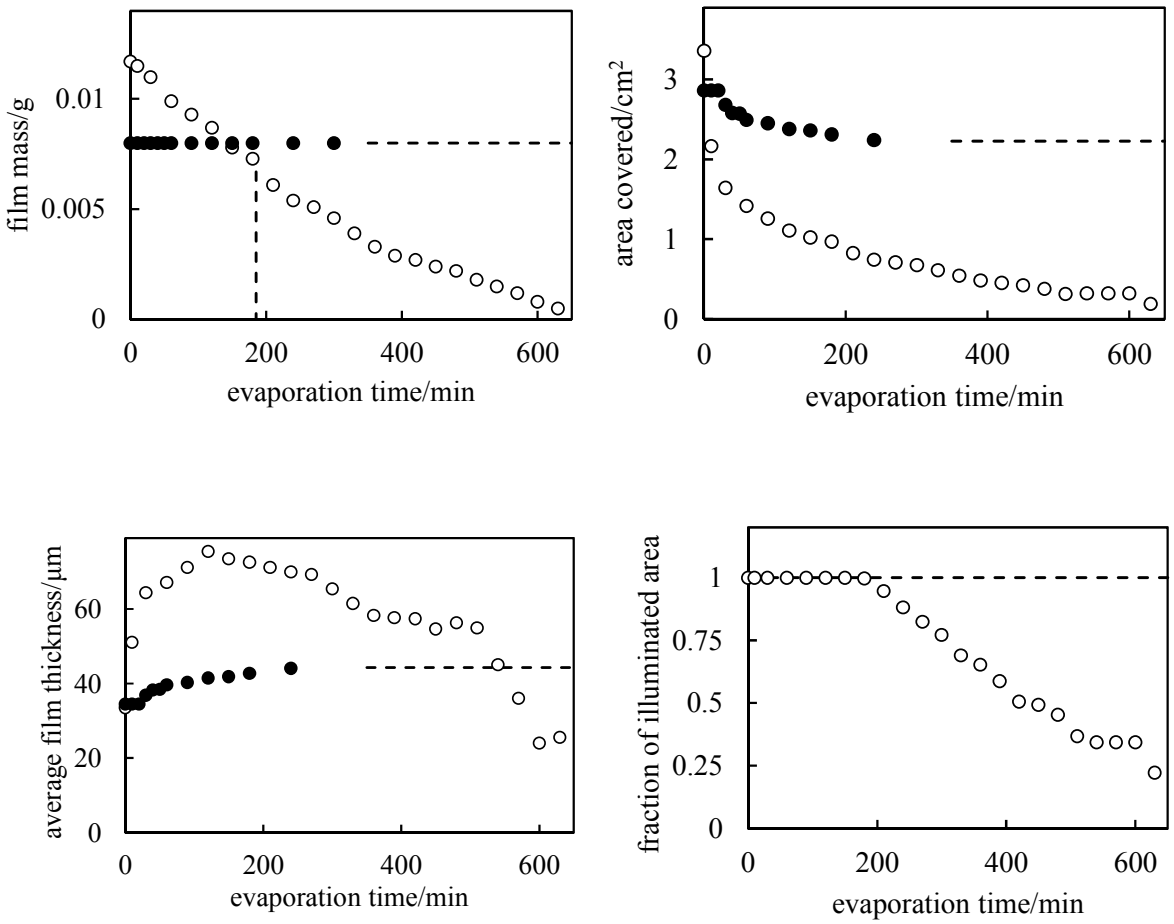

Figure 3. Variation of peak absorbance values (at 354 nm for squalane and 361 nm for PG versus air reference) with evaporation time for films containing 8 mM AVB in squalane or PG. The absorbance values of the quartz plate plus PG or squalane film without AVB are both 0.033. The horizontal dashed line indicates the long-time behaviour of the squalane film (measured at 1440 min).

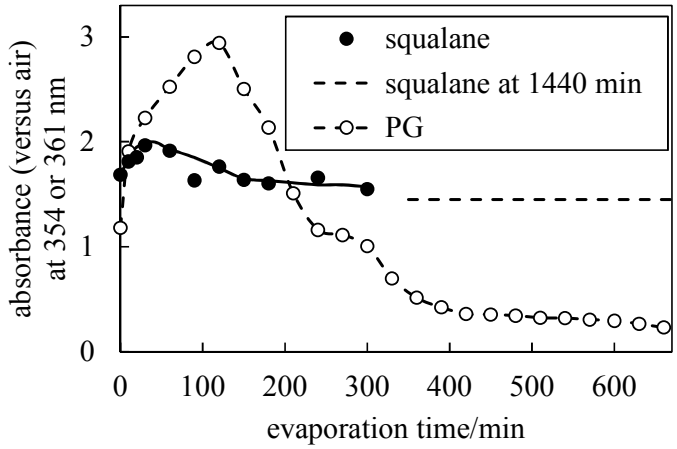

Figure 4. Variation of film mass, area and average thickness for particle-stabilised emulsion films initially containing equal volumes of SQ and PG and 4 mM AVB in the total emulsion (initially dissolved in the PG phase). PG-in-SQ emulsions were stabilised using 1 wt% of 23% SiOH silica particles; SQ-in-PG emulsions were stabilised using 1 wt% of 35% SiOH silica particles.

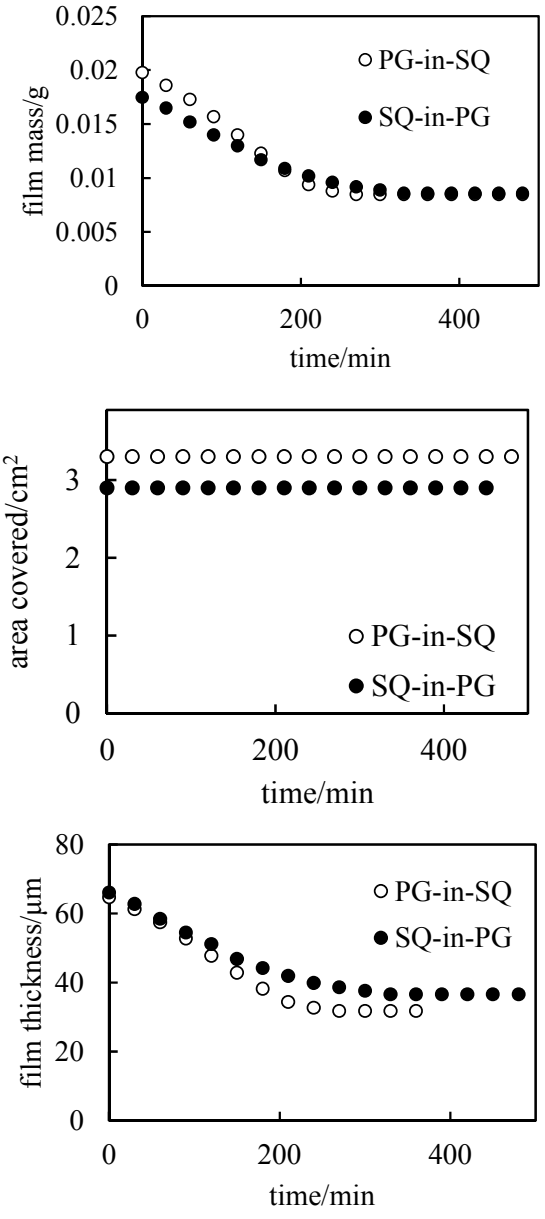

Figure 5. Optical micrographs of PG-in-SQ emulsion films during their evaporation. The emulsion films initially contained equal volumes of SQ and PG and 4 mM AVB in the total emulsion (initially dissolved in the PG phase) and were stabilised using 1 wt% of 23% SiOH silica particles;

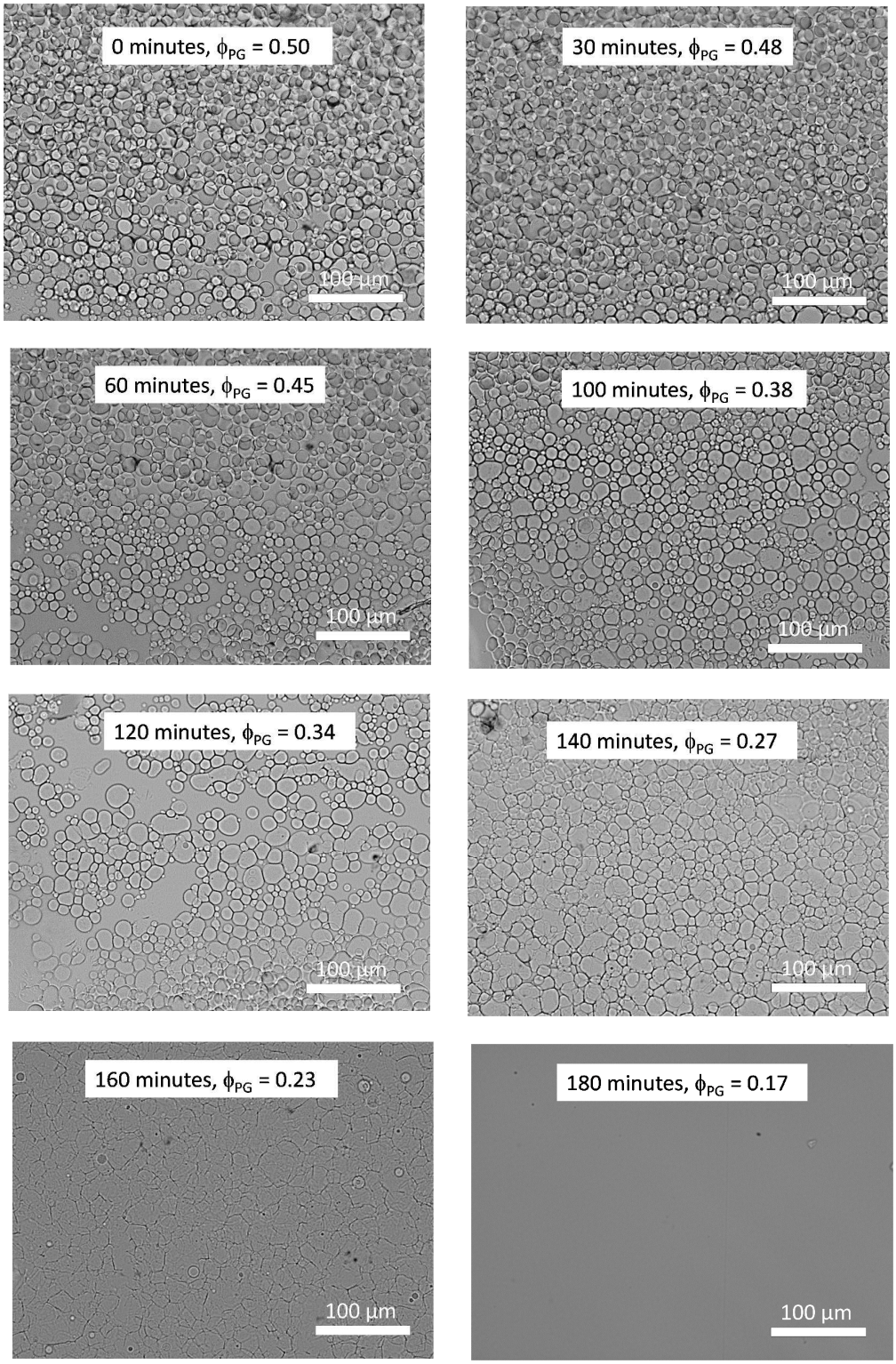

Figure 6. Optical micrographs of SQ-in-PG emulsion films during their evaporation. The emulsion films initially contained equal volumes of SQ and PG and 4 mM AVB in the total emulsion (initially dissolved in the PG phase) and were stabilised using 1 wt% of 35% SiOH silica particles.

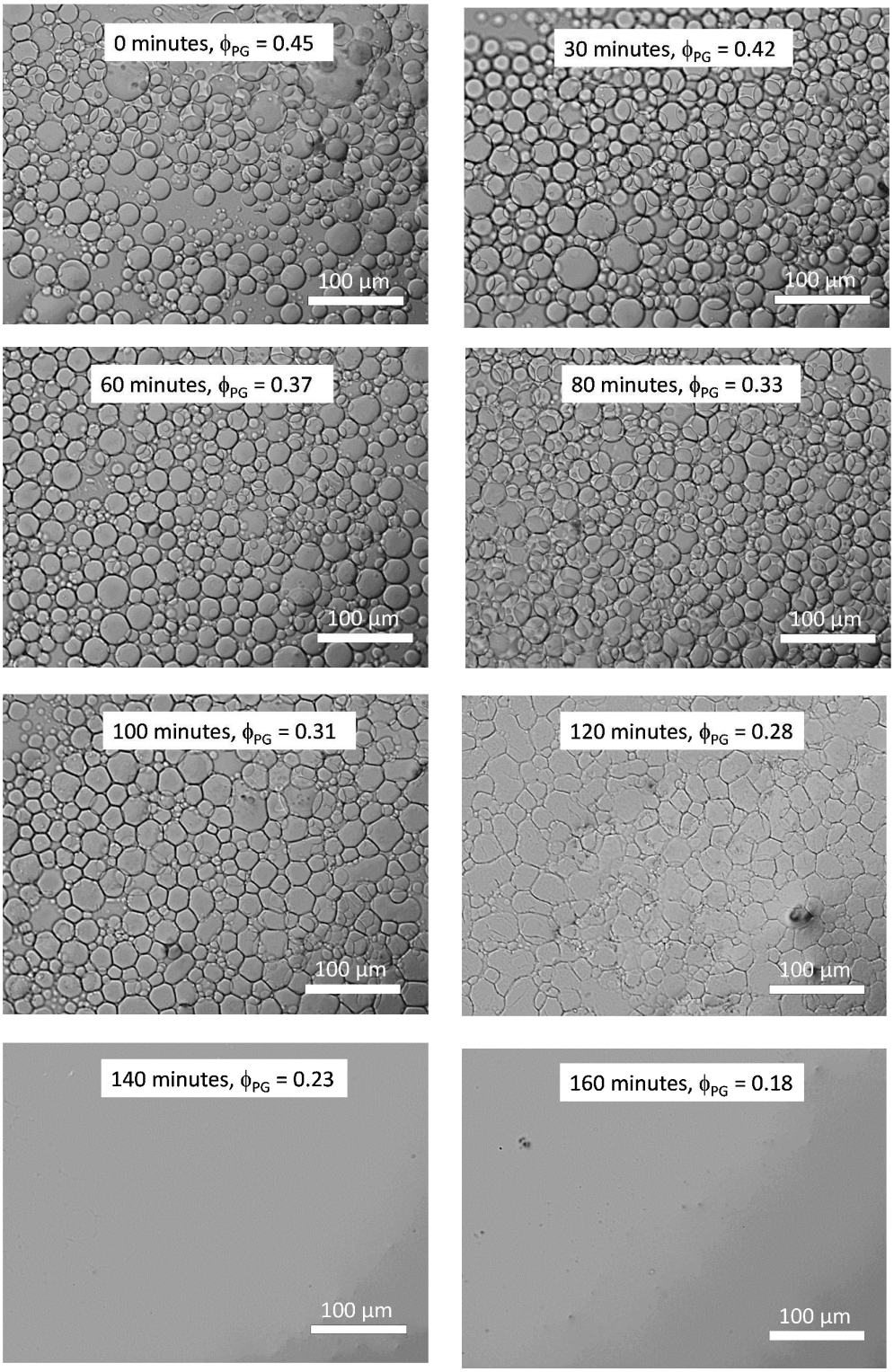

Figure 7. Measured (upper plot) and calculated (middle plot) UV specular spectra versus air as reference during evaporation of a PG-in-SQ emulsion film initially with 19.8 mg mass and containing equal volumes of SQ and PG and 4 mM AVB in the total emulsion (initially dissolved in the PG phase). The film was stabilised using 1 wt% of 23% SiOH silica particles. The inset plots show absorbance at 360 nm versus evaporation time in minutes. The lower plot shows the variation of calculated and measured SPF based on the specular and diffuse absorbances.

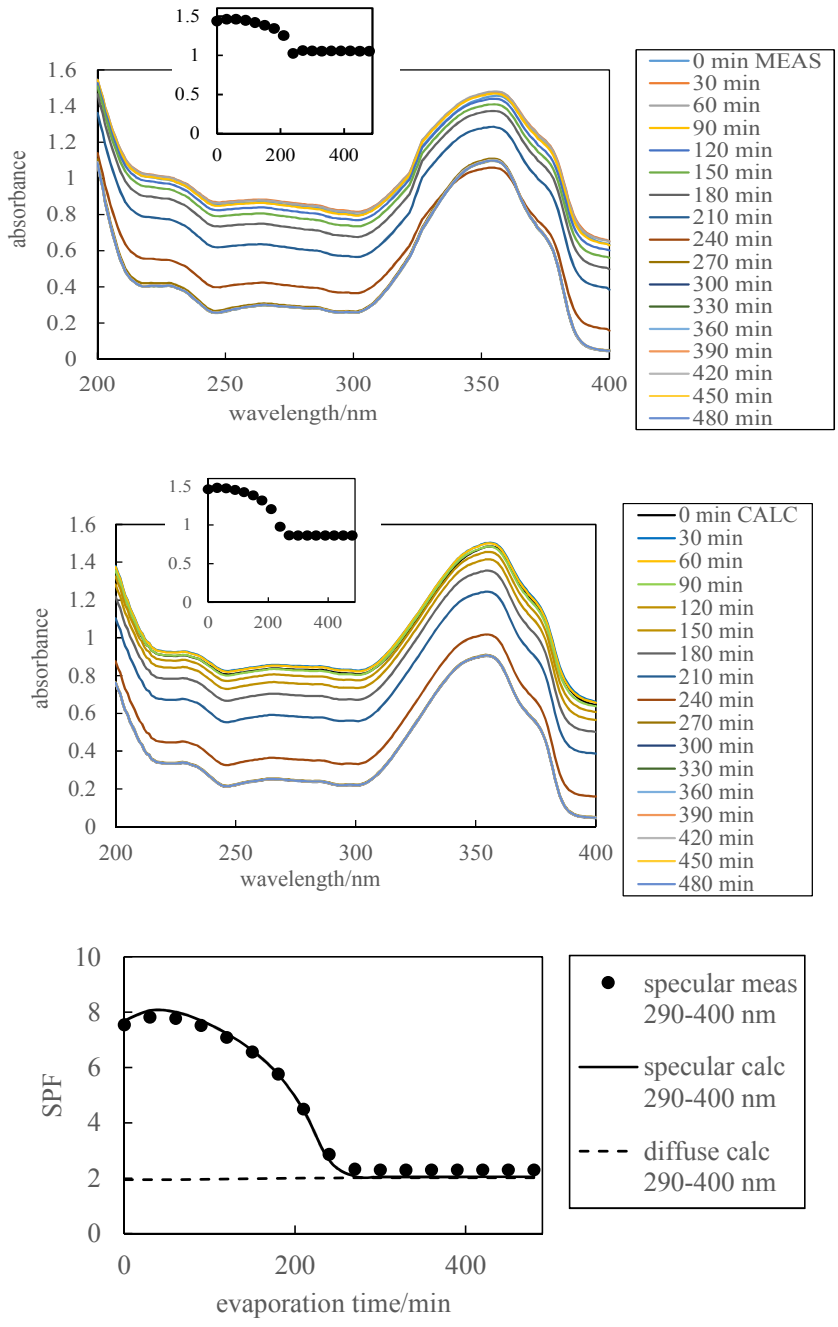

Figure 8. Measured (upper plot) and calculated (middle plot) UV specular spectra versus air as reference during evaporation of a SQ-in-PG emulsion film initially with 17.5 mg mass and containing equal volumes of SQ and PG and 4 mM AVB in the total emulsion (initially dissolved in the PG phase). The film was stabilised using 1 wt% of 35% SiOH silica particles. The inset plots show absorbance at 360 nm versus evaporation time in minutes. The lower plot shows the variation of calculated and measured SPF based on the specular and diffuse absorbances.

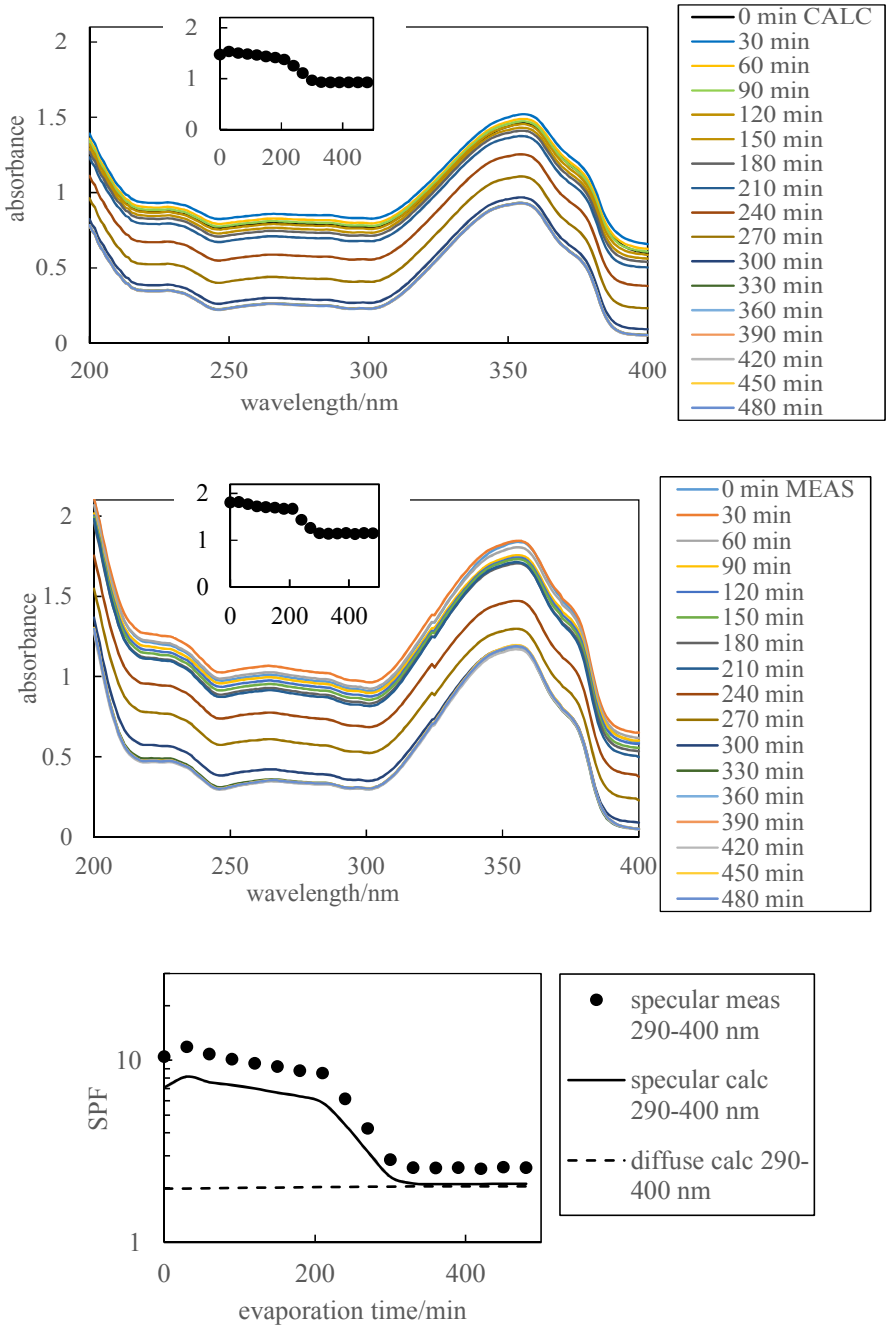

Figure 9. Variation of film mass, area, average thickness and fraction of illuminated area covered (A_f) with evaporation time for a decane-in-PG film initially containing equal volumes of decane and PG and 4 mM AVB. The film was stabilised by 1 wt% of 23% SiOH silica particles.

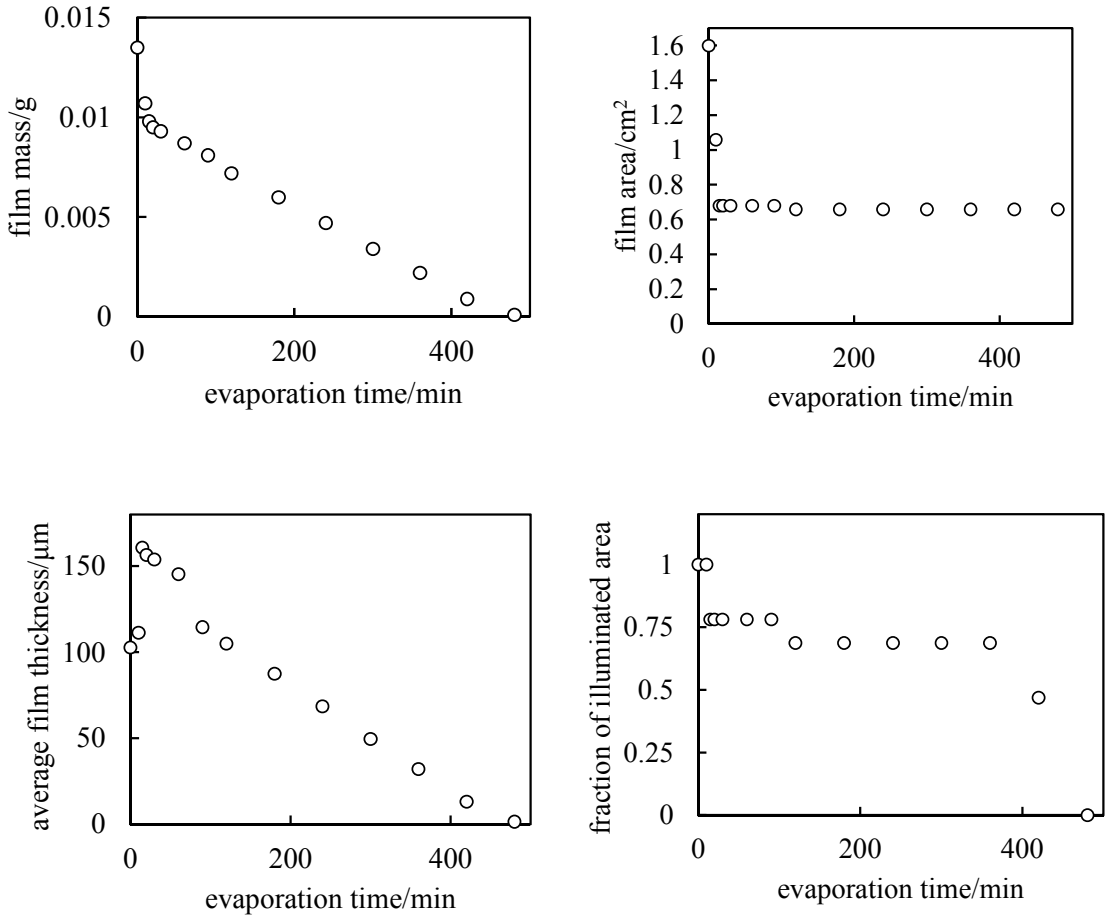

Figure 10. Representative images of an evaporating film of a decane-in-PG emulsion initially containing equal volumes of decane and PG with 4 mM AVB overall (initially 1.65 mM in PG and 6.35 mM in decane). The emulsion was stabilised by 1 wt% of 23% SiOH silica particles.

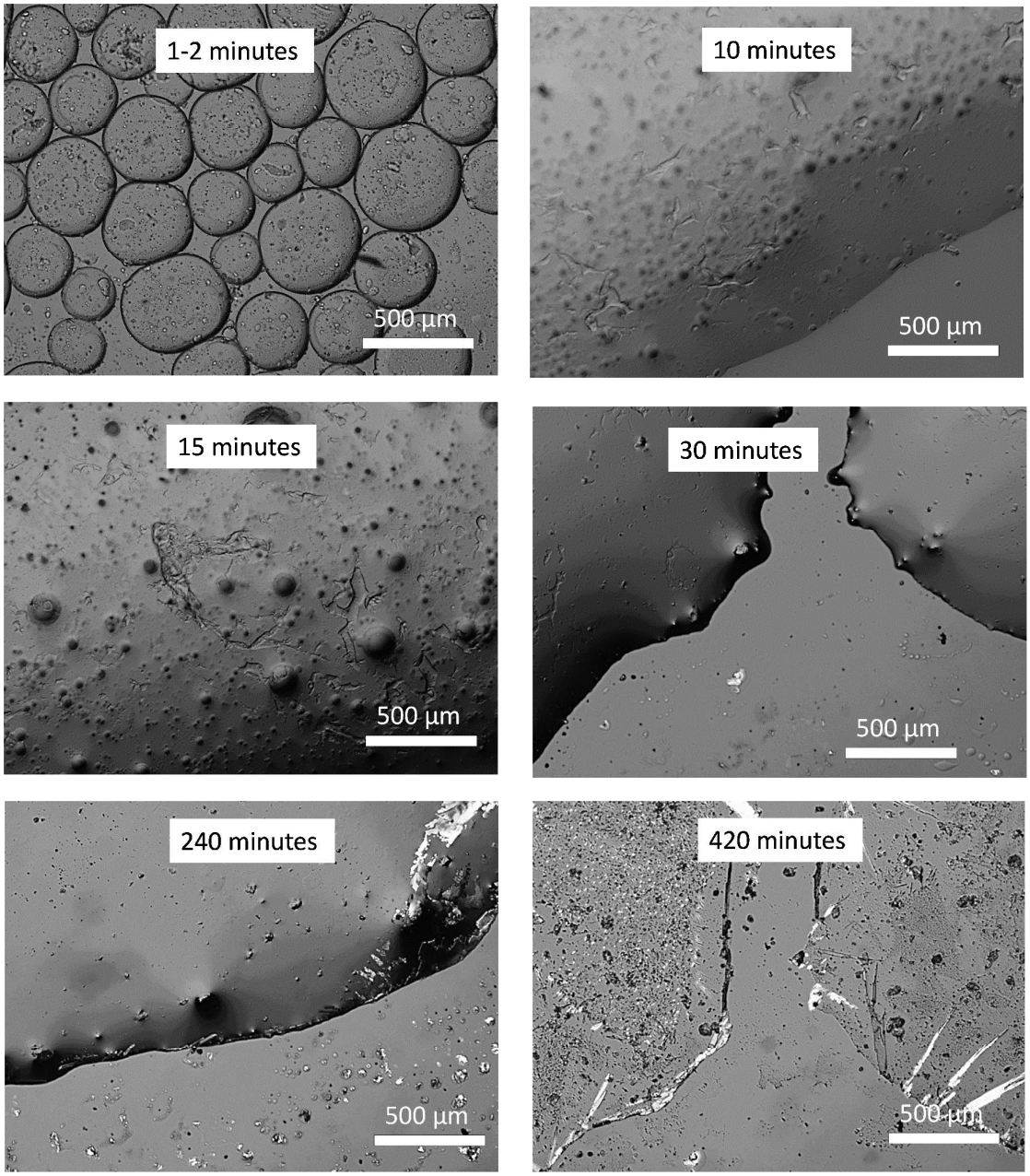

Figure 11. Measured (upper plot) and calculated (lower plot) UV specular spectra versus air as reference during evaporation of a decane-in-PG emulsion film initially containing equal volumes of decane and PG and 4 mM AVB in the total emulsion (initially dissolved in both phases at their equilibrium concentrations). The film was stabilised using 1 wt% of 23% SiOH silica particles. The middle plot shows the variation of the measured specular absorbance at 400 nm with evaporation time.

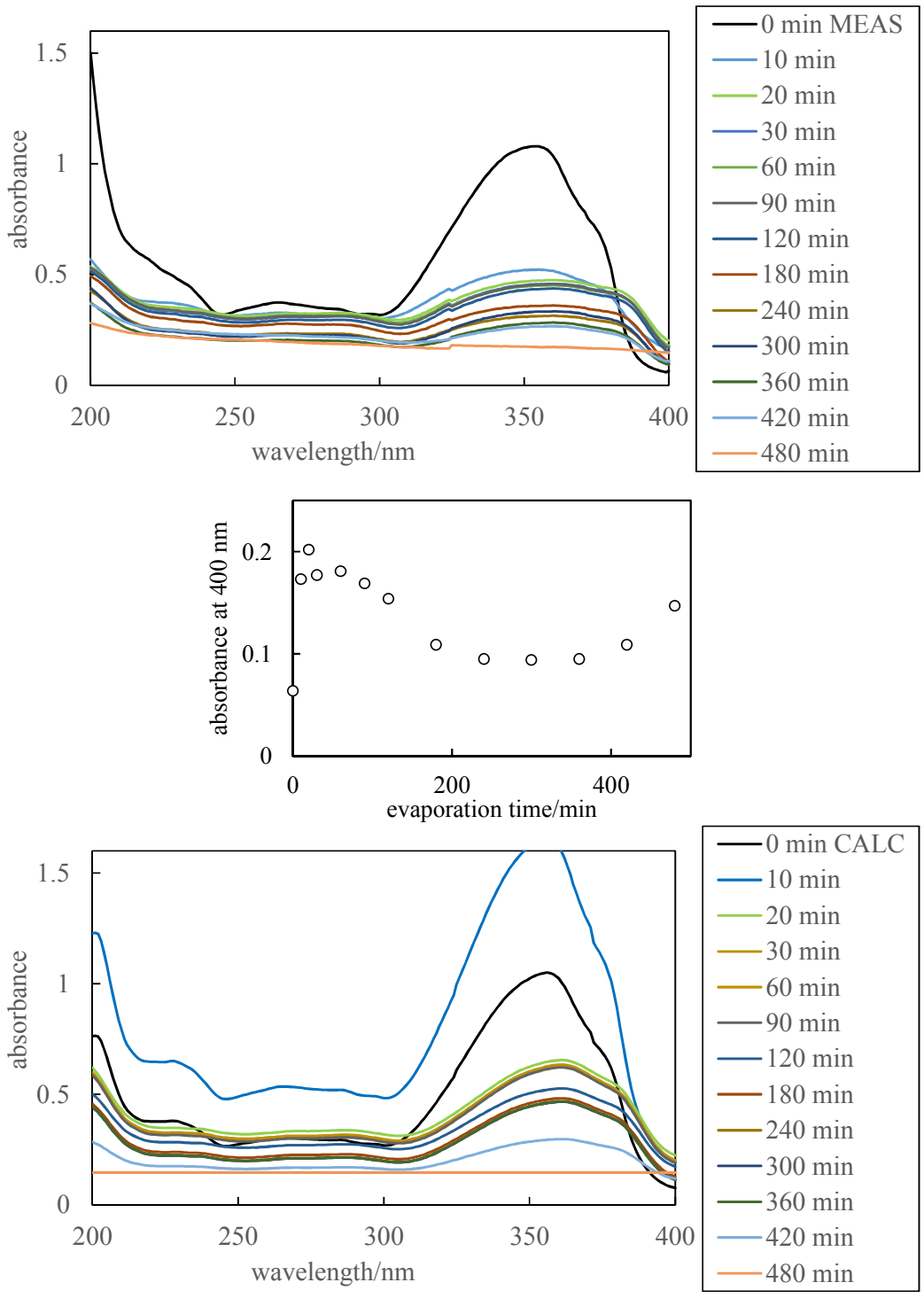

Table of Contents/Abstract Graphic

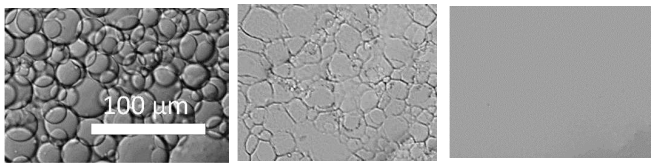

Particle-stabilised SQ-in-PG emulsion film after (left to right) 30, 120 and 140 minutes evaporation.